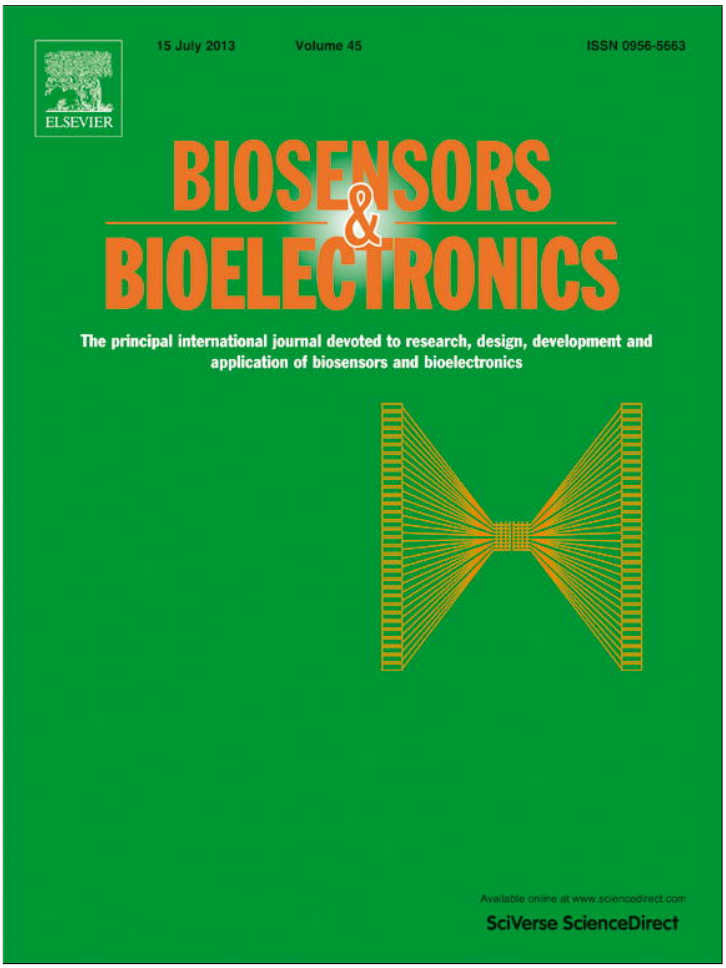

Biosensors and Bioelectronics 45 (2013) 195–200

Contents lists available at SciVerse ScienceDirect

Biosensors and Bioelectronics

journal homepage: www.elsevier.com/locate/bios

# Signal amplification for electrochemical immunosensing by in situ assembly of host–guest linked gold nanorod superstructure on immunocomplex

Dajie Lin [a], Jie Wu [a], Huangxian Ju [a,*], Feng Yan [b,*]

[a] State Key Laboratory of Analytical Chemistry for Life Science, Department of Chemistry, Nanjing University, Nanjing 210093, PR China
[b] Jiangsu Institute of Cancer Prevention and Cure, Nanjing 210009, PR China

ARTICLE INFO

*Article history:*
Received 22 November 2012
Received in revised form
30 January 2013
Accepted 31 January 2013
Available online 13 February 2013

*Keywords:*
Immunoassay
Signal amplification
Electrochemistry
Host–guest linking
Gold nanorod
Tumor marker

ABSTRACT

An amplification strategy for signal tracing was developed by introducing a host–guest binding reaction into the assembly process of gold nanorods (AuNRs) superstructure. The amplification pathway firstly used a thio-β-cyclodextrin (SH-β-CD) functionalized gold nanoparticles to label signal antibody, and then in situ assembled multi-layer SH-β-CD end-functionalized AuNRs to sandwich immunocomplex on immunosensor surface by using 4,4,4,4-(21H, 23H-porphine-5,10,15,20-tetrayl) tetrakis (benzoic acid) as a bridge to achieve simple and convenient host–guest reaction. The built end-to-end AuNRs superstructure showed excellent performance for the signal amplification in connection with the electrochemical biosensing by preoxidation and then voltammetric analysis of gold element. Using α-fetoprotein as an analyte, the immunosensor was constructed by covalently binding capture antibody to chitosan–carbon nanotubes-poly(diallyldimethylammonium chloride) modified electrode. The superstructure rich in AuNRs brought an enhanced detection sensitivity of protein, which could detect α-fetoprotein in a linear range from 0.5 pg $mL^{-1}$ to 0.5 ng $mL^{-1}$ with a detection limit down to 0.032 pg $mL^{-1}$. The immunoassay exhibited good stability and acceptable reproducibility and accuracy. The in situ superstructure assembly could be extended to other labeled recognition systems, providing a promising novel avenue for signal amplification and potential applications in bioanalysis and clinical diagnostics.



## 1. Introduction

Controllable assembly of nanoscale building blocks has been one of the most exciting and active research areas in nanoscience and nanotechnology (Huang et al., 2001). These assemblies can exhibit unique synergistic properties and are widely applied in biosensing, nanoscale electronic and optical devices (Caswell et al., 2003; Wang et al., 2010). Due to the urgent need of sensitive, rapid and reliable methods for biomarkers detection (Ferrari, 2005; Stoeva et al., 2006; Wu et al., 2007), electrochemical immunoassay has been well developed by different signal amplification strategies (Nie et al., 2009; Malhotra et al., 2010). The amplification pathway is generally constructed by loading high ratio of signal or signal-related molecule to reporting element on one nanocarrier to trace the immunoreaction (Wang et al., 2004; Mani et al., 2009; Du et al., 2011; Teng et al., 2011). Enzymes and some enzyme mimics benefiting of their unique catalytic ability are the most popular signal-related molecules, and have been extensively loaded on various nanocarriers to form signal probes for construction of ultrasensitive immunoassays (Wang et al., 2004; Mani et al., 2009; Du et al., 2011). Metal and semiconductor nanoparticles (Wang et al., 2008; Ting et al., 2009; Ho et al., 2010; Lu et al., 2011; Peng et al., 2011) are also attractive electroactive labels because these nanomaterials can be measured by electrochemical stripping analysis, a highly sensitive detection technique. Gold and silver nanoparticles are the most used metal nanoparticles in electrochemical immunosensing due to their unique abilities of good biocompatibility and easy functionalization with proteins (Dequaire et al., 2000). In order to further enhance the detection sensitivity, gold nanoparticles (AuNPs) have been congregated together (Wang et al., 2008) or assembled on another nanocarrier to label the signal antibody (Ting et al., 2009). However, such processes are normally accompanied with complicated procedures and some synthesized probes are unstable. Thus the in situ formation of superstructure assemblies on the immunocomplex is a good candidate way for amplifying the voltammetric stripping signal. This work designed a novel superstructure assembly avenue by a host–guest reaction of end-

* Corresponding author. Tel./fax: +86 25 83593593.
*E-mail addresses:* hxju@nju.edu.cn (H. Ju), yanfeng2007@sohu.com (F. Yan).

0956-5663/$ - see front matter © 2013 Elsevier B.V. All rights reserved.
http://dx.doi.org/10.1016/j.bios.2013.01.070

functionalized gold nanorod (AuNRs) with a bridge molecule as linker.

The aggregation of AuNRs has been proposed by biotin–streptavidin connectors, which can be performed with biotin-functionalized AuNRs and streptavidin as a linker (Caswell et al., 2003; Katz and Willner, 2004). Similarly DNA-coated AuNRs have been assembled to form three-dimensional AuNRs aggregates through the addition of a complementary linker DNA (Dujardin et al., 2001; Katz and Willner, 2004). Recently some molecular biological techniques such as DNA hybridization (Li et al., 2011) and rolling circle amplification (RCA) (Hsu and Huang, 2004; Hu and Zhang, 2010) have been introduced into the formation of three-dimensional aggregates of metal nanoparticles, which leads to several methods for signal amplification. All these methods involve the use of proteins or DNA, thus have some intrinsic drawbacks, including easy denaturation and time-consuming preparation (Lee et al., 2011). Here the aggregation of AuNRs was achieved by host–guest reaction between thio-β-cyclodextrin (SH-β-CD, to act as host) end-functionalized AuNRs (CD–AuNRs) and 4,4,4,4-(21H, 23H-porphine-5,10,15,20-tetrayl) tetrakis (benzoic acid) (TCPP, to act as guest and a chemical linker by forming a trans-type 1:2 complex) (Kano et al., 2002) to avoid these drawbacks. The in situ assembled superstructure had been for the first time used to amplify the detectable signal for immunoassay.

Supramolecular assembly encompasses the formation of structurally well-defined aggregates with fast kinetics, good specificity and stability (Uhlenheuer et al., 2010). The diffusion-controlled assembly process is much faster than those of bioorthogonal covalent reactions (Agasti et al., 2012). After the sandwich immunocomplex was formed to attach SH-β-CD functionalized gold nanoparticle labeled signal antibody (CD–AuNP-$Ab_2$), multi-layer CD–AuNRs could be efficiently assembled on the immunosensor surface by combining the advantage of host–guest assembly through a strong van der Waals force. The end-to-end AuNRs superstructure greatly amplified the voltammetric stripping signal of AuNRs associated with the antigen concentration (Scheme 1). With α-fetoprotein (AFP) as an analyte, the proposed method showed a detection limit down to sub pg $mL^{-1}$ level, which was lower than those of pg $mL^{-1}$ level using nanomaterial-based multi-enzyme labels for immunoassays (Wang et al., 2004; Mani et al., 2009; Du et al., 2011). Thus the host–guest assembly could be a promising signal amplification avenue for highly sensitive bioanalysis.

## 2. Materials and methods

### 2.1. Materials and reagents

Capture antibody ($Ab_1$) and $Ab_2$ of AFP (clone nos. A14C11 and A46C9) were purchased from Shuangliu Zhenglong Biochem. Lab (Chengdu, China). Bovine serum albumin (BSA), chitosan, and PDDA (20%, w/w in water, MW: 200,000–350,000) were purchased from Sigma-Aldrich (USA). Cetyltrimethylammonium bromide (CTAB, 98%), TCPP were purchased from Alfa Aesar. Chloroauric acid ($HAuCl_4 \cdot 4H_2O$), trisodium citrate, and silver nitrate ($AgNO_3$) were obtained from Shanghai Reagent Company (Shanghai, China). Sodium borohydride ($NaBH_4$) was obtained from Sinopharm Chemical Reagent Co. Ltd (China). Thio-β-cyclodextrin (SH-β-CD) was commercially available from Shandong Binzhou Zhiyuan Bio-Technology Co., Ltd (Shangdong, China). AFP standard solutions from 0 to 75 ng $mL^{-1}$ were from AFP ELISA kit, which was supplied by Fujirebio Diagnostics AB (Göteborg, Sweden). Ultrapure water obtained from a Millipore water purification system ($\geq$18 MΩ, Milli-Q, Millipore) was used in all assays. The clinical serum samples were from Jiangsu Institute of Cancer Research. All other reagents were of analytical grade and used as received. Phosphate buffered saline (PBS, 0.02 M) with various pHs were prepared by mixing the stock solutions of $NaH_2PO_4$ and $Na_2HPO_4$. The washing buffer was PBS (0.02 M, pH 7.4) containing 0.05% (w/v) Tween-20 (PBST).

### 2.2. Apparatus

The morphology of the AuNRs was examined using a JEM 2100 high-resolution TEM (Japan). Scanning electron microscopic (SEM) images were obtained using a Hitachi S-4800 scanning electron microscope (Japan). The UV–vis absorption spectrum was observed with a UV-3600 UV–vis spectrophotometer (Shimadzu, Japan). All electrochemical immunoassays were performed on a CHI 660D electrochemical workstation (Chenhua, Shanghai, China). The reference levels of AFP in the human serum samples were detected with an automated electrochemiluminescent analyzer (Elecsys 2010, Roche).

### 2.3. Preparation of CD–AuNP-$Ab_2$

The CD–AuNP-$Ab_2$ was prepared according to a previous report with slight modification (Stoeva et al., 2006; Lin et al., 2011). As shown in Scheme 1A, after adjusting the pH of 3 mL of 4 nM Au colloidal solution (supplementary information) to 9.2, 9 μL of 1.3 mg $mL^{-1}$ $Ab_2$ was added to the solution, followed by incubation at 10 °C for 4 h with gentle stirring. A 0.2 mL portion of 5 μM SH-β-CD was then added to the resulting solution. After stirring for 10 h, 0.1 mL of PBS containing 1% BSA was dropped into the suspension, followed by a gentle stirring at 4 °C for 2 h. Afterwards, the excess antibodies and SH-β-CD were removed by centrifugation at 12,000 rpm for 20 min, and the precipitate was redispersed in 10 mM PBS, this procedure was repeated thrice. The obtained CD–AuNP-$Ab_2$ was redispersed in 2 mL of 10 mM pH 7.4 PBS and stored at 4 °C.

### 2.4. Preparation of CD–AuNRs

For the preparation of CD–AuNRs (Scheme 1B), 0.2 mL of 5 μM SH-β-CD was added dropwise into 2 mL of AuNRs (supplementary information) with stirring. After the mixture was gently shaken at room temperature for 4 h, the formed CD–AuNRs were collected by thrice centrifugation at 8000 rpm for 15 min with 5 mM CTAB as the washing solution. Finally, the functionalized AuNRs were redispersed in 2 mL of 5 mM CTAB solution and stored at 4 °C.

### 2.5. Fabrication of immunosensor

The glassy carbon electrode (GCE) with 3-mm diameter was polished to a mirror using 1.0, 0.3 and 0.05 μm alumina slurry (Buehler), followed by rinsing thoroughly with deionized water. After successive sonication in 1:1 nitric acid, acetone and deionized water, the electrode was rinsed with water and allowed to dry at room temperature. As shown in Scheme 1C, 5 μL of 1 mg $mL^{-1}$ PDDA/CNTs solution (supplementary information) was dropped on the pretreated GCE, which was dried in air. Then, 5 μL of 0.05% chitosan solution was dropped on the film and dried in air. The modified electrode was washed with water and incubated with 5 μL of 2.5% glutaraldehyde (in 50 mM PBS, pH 7.4) for 2 h, followed by washing with water. 5 μL of 0.3 mg $mL^{-1}$ $Ab_1$ of AFP was then dropped onto the surface, which was incubated at room temperature for 60 min and 4 °C overnight in a 100% moisture-saturated environment. Subsequently, excess antibody was removed with pH 7.4 PBST and PBS, respectively. Finally, 5 μL of PBS containing 5% BSA was dropped on the electrode surface and incubated for 60 min at room temperature to block possible remaining active sites against nonspecific adsorption. After another washing with pH 7.4 PBST and PBS, the immunosensor was obtained.

### 2.6. Measurement procedure

To carry out the immunoreaction and electrochemical measurements, the immunosensor was firstly incubated with 5 μL of AFP standard solution or serum sample for 50 min at 37 °C. After washing with washing buffer and pH 7.4 PBS, the immunosensor was further incubated with 5 μL of CD–AuNP-$Ab_2$ for 30 min at 37 °C. The immunosensor was further incubated with 5 μL of 10 nM TCPP for 25 min at 37 °C and then 5 μL of CD–AuNRs for 25 min at 37 °C to assemble the first layer of AuNRs (Scheme 1C). By incubation with TCPP and CD–AuNRs alternately, multi-layer AuNRs could be in situ assembled on the immunosensor surface

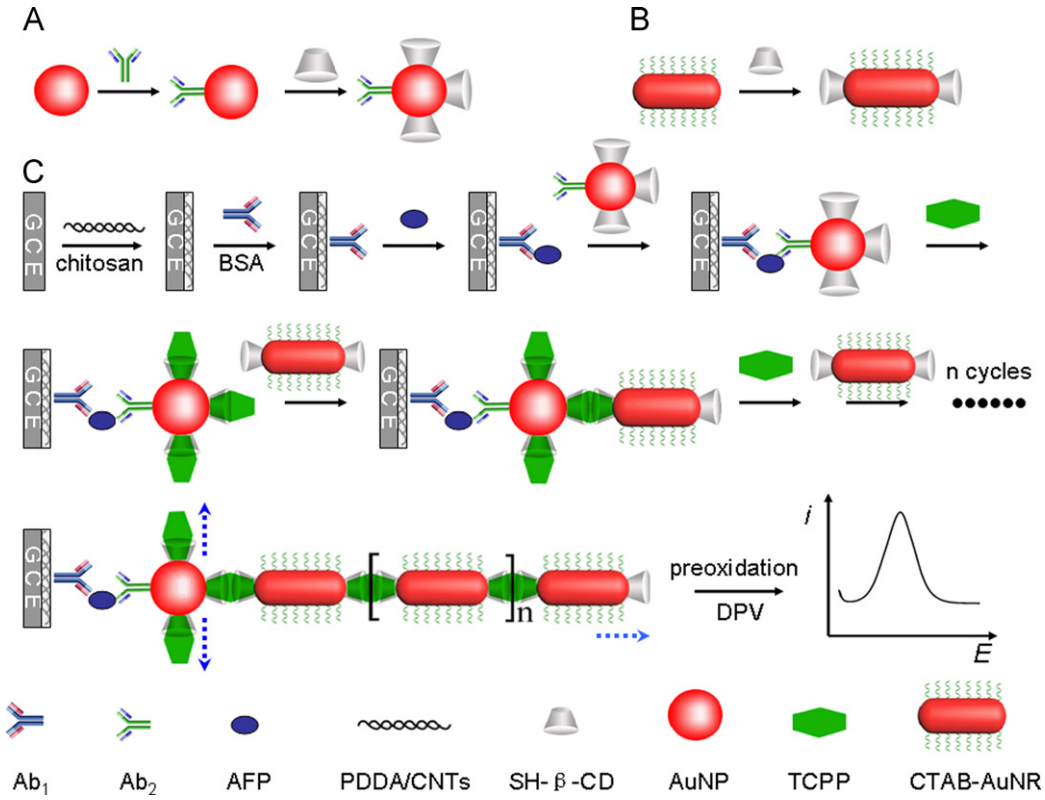


**Scheme 1.** Schematic representation of the preparation of (A) CD-$Ab_2$/AuNPs and (B) CD/AuNRs tags; (C) Immunosensor fabrication and sandwich-type immunoassay with AuNRs superstructure based signal amplification.

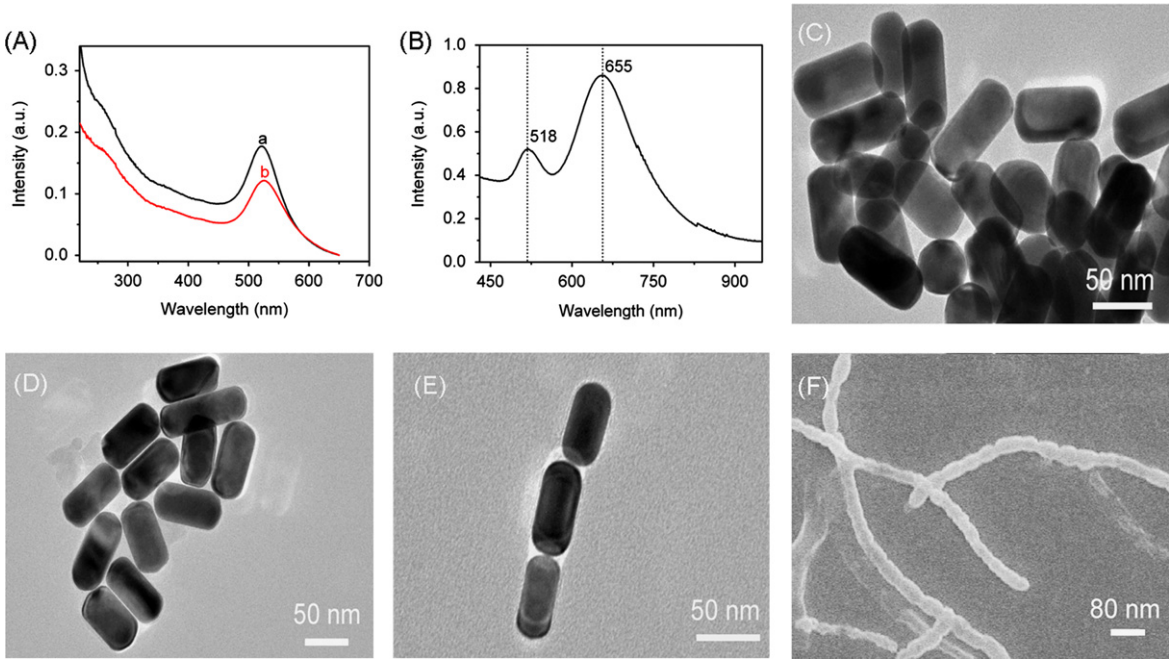


**Fig. 1.** UV–vis spectra of (A) AuNPs (curve a) and CD-$Ab_2$/AuNPs (curve b), and (B) AuNRs; TEM images of (C) AuNRs, (D) CD/AuNRs and (E) AuNRs assembly; (F) SEM image of AuNRs assembly.

through the host–guest interaction between CD and TCPP. Finally, the immunosensor was placed in 0.1 M HCl solution to perform the electrochemical oxidation of AuNRs at a constant potential of +1.60 V for 60 s, and immediately differential pulse voltammetric (DPV) detection was performed from +0.68 to +0.28 V at 50 mV/s with a pulse amplitude of 50 mV and a width of 50 ms.

## 3. Results and discussion

### 3.1. Characterization of CD–AuNP-$Ab_2$ and CD–AuNRs

The size of AuNPs can be estimated from UV–vis spectrum. As shown in Fig. 1A, the UV–vis spectrum of AuNPs showed an absorption peak at 520 nm (curve a), which corresponded to a diameter of about 20 nm (Xia et al., 2010). Compared with AuNPs, the UV–vis spectrum of CD–AuNP-$Ab_2$ showed a red shift of the absorption peak to 526 nm (curve b), which was attributed to the presence of protein, indicating the successful loading of $Ab_2$ on AuNPs.

The AuNRs were synthesized according to the seed-mediated growth approach with the help of the shape-directing surfactant of CTAB (Caswell et al., 2003; Wang et al., 2010; Ye et al., 2012). The obtained AuNRs were stable and soluble in water, and their side surfaces rather than the end surfaces could be covered with at least a bilayer of CTAB (Caswell et al., 2003; Ye et al., 2012). The UV–vis spectrum of AuNRs exhibited two distinct and narrow plasmon resonance bands centered at 518 and 655 nm, which were assigned to the typical traverse and longitudinal plasmon resonances of AuNRs (Kim et al., 2002), respectively (Fig. 1B), indicating the successful formation of AuNRs with good monodispersity. TEM image indicated that the AuNRs were quite uniform in shape and size (Fig. 1C). The average length and aspect ratio of AuNRs were 78 nm and 2, respectively. Based on the strong and specific binding between –SH group and gold atom, the SH-β-CD could be easily bound on the exposed end surfaces of AuNRs to form CD–AuNRs (Caswell et al., 2003). No significant difference was observed between the morphologies of AuNRs and CD–AuNRs (Fig. 1D). The formation of CD–AuNRs was further characterized by mass spectrometry (Fig. S1). Compared with AuNRs (Fig. S1B), the CD–AuNRs (Fig. S1C) showed the same peaks as free SH-β-CD (Fig. S1A) at *m/z* 1173, 1196 and 1214 (Fig. S1C), which were corresponding to $[SH\text{-}CD+Na]^+$, $[SH\text{-}CD+2Na-H]^+$, and $[SH\text{-}CD+2Na+H_2O-H]^+$, respectively, indicating the successful modification of SH-β-CD on AuNRs. As the SH-β-CD was linked on the end surfaces of AuNRs, the AuNRs would predominately end-to-end bind in the presence of TCPP to form end-to-end assemblies. TEM and SEM images showed the formation of end-to-end assemblies of AuNRs upon the addition of TCPP in CD–AuNRs (Fig. 1E and F).

### 3.2. Characterization of immunosensor

Carbon nanotubes (CNTs) possess high conductivity and can facilitate electron transfer on electrode surface, thus have been widely used in the construction of biosensors. Here, the SEM image

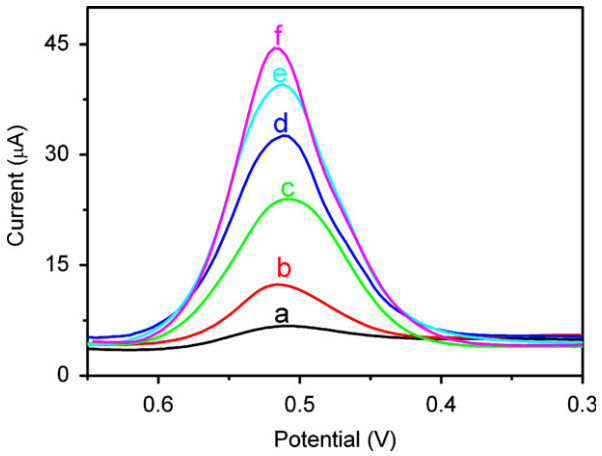


**Fig. 3.** DPV responses of immunosensors after sandwich incubation with 0 (a) or 50 pg/mL AFP (b to f), and CD-$Ab_2$/AuNPs, followed by in situ assembly of 0 (a, b), 1 (c), 2 (d), 3 (e), and 4 (f) generations of AuNRs through host–guest interaction between CD and TCPP.

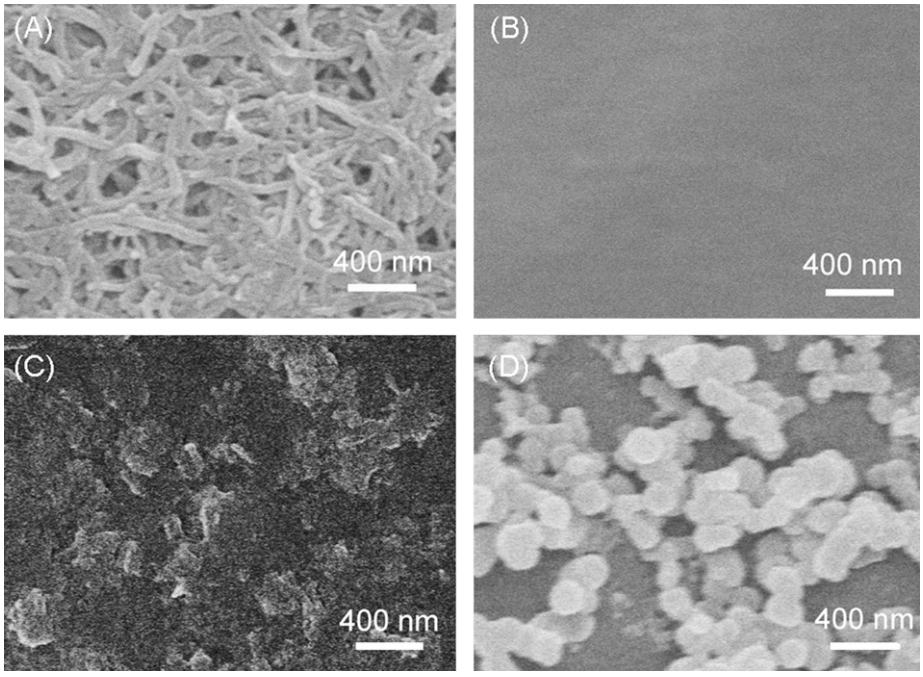


**Fig. 2.** SEM images of (A) PDDA/CNTs/GCE, (B) chitosan/PDDA/CNTs/GCE, (C) immunosensor, and (D) AuNRs assemblies on immunocomplexes.

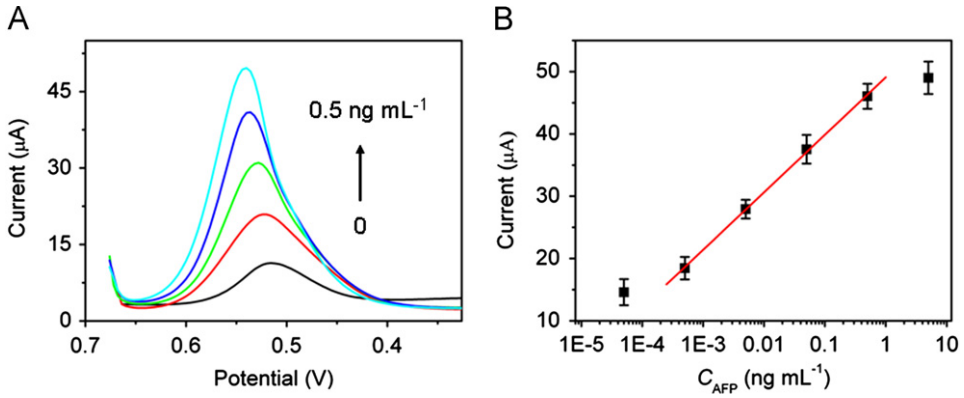


**Fig. 4.** DPV responses (A) and calibration curve (B) of immunosensor for the detection of AFP at concentrations of 0, 0.5, 5 and 50 pg/mL, and 0.5 ng/mL, respectively (error bars were obtained by thrice repetitive measurements).

of PDDA/CNTs film displayed a well-dispersed structure of small bundle or single tubes with diameters of 30–40 nm (Fig. 2A). The coating of chitosan on the PDDA/CNTs film led to a smoother and more uniform surface topography (Fig. 2B). After $Ab_1$ was immobilized on the chitosan/PDDA/CNTs modified GCE by glutaraldehyde cross-linking, an obvious aggregation of the trapped biomolecules could be observed (Fig. 2C), indicating the successful binding of $Ab_1$ on chitosan/PDDA/CNTs modified GCE and the successful fabrication of immunosensor. After a sandwich immunoreaction with 50 pg $mL^{-1}$ AFP and CD–AuNP-$Ab_2$, and then alternative incubation with CD–AuNRs and TCPP, obvious aggregation of AuNRs was observed on the surface of immunosensor (Fig. 2D), indicating the successful formation of AuNRs superstructure on the immunosensor through the host–guest interaction between CD and TCPP. Due to the different states of the CD–AuNP sites embedded in the chitosan/proteins (immunocomplex) membrane, the assembly rate of the host–guest superstructure at different sites is different, leading to the irregular sizes of the AuNRs assemblies.

### 3.3. Immunoassay and signal amplification at immunosensor

The preparation process of the immunosensor and the detection strategy with sandwich-type electrochemical immunoassay was shown in Scheme 1. After sandwich-type immunoreactions, the CD–AuNP-$Ab_2$ was captured on the surface of the immunosensor by the formation of immunocomplex. With further alternative incubation with CD–AuNRs and TCPP, the CD–AuNRs would be end-to-end assembled to CD–AuNP-$Ab_2$ by CD–TCPP based host–guest interaction. Finally, the AuNRs assemblies were electrochemical oxidized in 0.1 M HCl solution, and immediately the DPV detection was performed to record the reduction signal for immunoassay.

Fig. 3 shows the DPV responses of the immunosensor in 0.1 M HCl after sandwich immunoreaction and assembly of AuNRs with different numbers of generation. Compared with the background response (curve a), the immunosensor sandwiched with 50 pg $mL^{-1}$ target and CD–AuNP-$Ab_2$ showed an obvious DPV response (curve b), indicating the association of CD–AuNP-$Ab_2$ on the immunosensor. Furthermore, the in situ assembly of AuNRs through alternative incubation with CD–AuNRs and TCPP led to enhanced DPV response, which depended on the number of generation for AuNRs assembly (curves c–f). The DPV response increased sharply in the first three generations, and trended to slow increase in the higher generations, along with the consideration of assembly time of 50 min for one generation. Considering the immunoassay time, this work performed the signal amplification with a three-generation assembly of AuNRs.

### 3.4. Analytical performance

Under the optimum conditions (Fig. S2), the DPV peak current of Au nanomaterials on the immunosensor increased with the increasing concentration of AFP in the incubation solution (Fig. 4). The calibration plot showed a good linear relationship between the DPV current and the logarithm of the analyte concentration in the range from 0.5 pg $mL^{-1}$ to 0.5 ng $mL^{-1}$ with a correlation coefficient of 0.9997 (Fig. 4B). The limit of detection at a signal-to-noise ratio of $3\sigma$ (where $\sigma$ is the standard deviation of signal in a blank solution) was 0.032 pg $mL^{-1}$, which was much lower than those reported previously (Ting et al., 2009; Du et al., 2011; Peng et al., 2011; Teng et al., 2011). Compared with traditional enzyme label amplification, the designed amplification strategy based on the in situ assembly of AuNRs superstructure possessed the advantages of easier operation and better stability. Furthermore, the sensitivity as the slope of the calibration plot for AFP was 5.75 μA•lg (mL $ng^{-1}$), which was 10 times larger than those of previously reported immunoassays with nanomaterial-carried enzyme amplification (Zhou et al., 2012). High sensitivity and low limit of detection could improve the detection precision and be suitable for detecting low-abundance biomarkers in serum samples, indicating great promise for practical application.

Both the intra-assay and inter-assay precisions of the immunosensors were examined with 5 immunosensors prepared with the same and different GCEs, respectively. At 50 pg $mL^{-1}$ AFP, the relative standard deviations (RSD) were 5.7% and 7.2%, respectively, showing the good precision and acceptable fabrication reproducibility. In addition, when the immunosensor was stored in dry at 4 °C, over 91% of the initial response was remained after a storage period of two weeks. These results indicated that the immunosensor had acceptable reliability and stability, and was suitable for the clinical detection of protein markers. Meanwhile, these results also highlighted the good stability of the proposed method.

### 3.5. Application in detection of serum tumor marker

The analytical reliability and application potential of the proposed method was evaluated by comparing the assay results of clinical serum samples using the proposed immunosensor with the reference values obtained by commercial electrochemiluminescent tests. Due to the high sensitivity, serum samples were appropriately diluted with 0.02 M pH 7.4 PBS prior to assay. The results showed an acceptable agreement with relative errors less than 11.5% (Table S1), indicating acceptable accuracy of the proposed method for the detection of AFP in clinical samples.

## 4. Conclusions

A new method for preparation of gold nanorods (AuNRs) superstructure and signal amplification was designed. The in situ assembly of multi-layer AuNRs superstructure on the immunocomplex attached on immunosensor surface was successfully achieved by SH-β-CD end-functionalized AuNRs and TCPP as a bridge linker, which was demonstrated with a series of techniques such as UV–vis spectroscopy, mass spectrometry, SEM and TEM. The gold superstructure tags could be electrooxidized in HCl for voltammetric stripping analysis, leading to a highly sensitive immunoassay method. This method showed a wide detection range and an ultralow detection limit for AFP. It exhibited convenient operability, high sensitivity, good stability and acceptable reproducibility and accuracy. By labeling different recognition elements with β-CD functionalized AuNPs, the in situ superstructure assembly could be extended to other recognition systems for more extensive analytical application. This work provided a promising novel avenue for signal amplification.

## Acknowledgments

We gratefully acknowledge the National Basic Research Program (2010CB732400), National Natural Science Foundation of China (21075055, 21135002, 21121091 and 21105046), PhD Fund for Young Teachers (20110091120012), the Leading Medical Talents Program from Department of Health of Jiangsu Province, and the Natural Science Foundation of Jiangsu (BK2011552).

## Appendix A. Supporting information

Supplementary data associated with this article can be found in the online version at http://dx.doi.org/10.1016/j.bios.2013.01.070.

## References

Agasti, S.S., Liong, M., Tassa, C., Chung, H.J., Shaw, S.Y., Lee, H., Weissleder, R., 2012. Angewandte Chemie International Edition 51, 450–454.
Caswell, K.K., Wilson, J.N., Bunz, U.H.F., Murphy, C.J., 2003. Journal of the American Chemical Society 125, 13914–13915.
Dequaire, M., Degrand, C., Limoges, B., 2000. Analytical Chemistry 72, 5521–5528.
Du, D., Wang, J., Lu, D.L., Dohnalkova, A., Lin, Y.H., 2011. Analytical Chemistry 83, 6580–6585.
Dujardin, E., Hsin, L.B., Wang, C.R.C., Mann, S., 2001. Chemical Communications, 1264–1265.
Ferrari, M., 2005. Nature Review Cancer 5, 161–171.
Ho, J.A., Chang, H.C., Shih, N.Y., Wu, L.C., Chang, Y.F., Chen, C.C., Chou, C., 2010. Analytical Chemistry 82, 5944–5950.
Hsu, H.Y., Huang, Y.Y., 2004. Biosensors and Bioelectronics 20, 123–126.
Hu, J., Zhang, C.Y., 2010. Analytical Chemistry 82, 8991–8997.
Huang, Y., Duan, X., Wei, Q., Lieber, C.M., 2001. Science 291, 630–633.
Kano, K., Nishiyabu, R., Asada, T., Kuroda, Y., 2002. Journal of the American Chemical Society 124, 9937–9944.
Katz, E., Willner, I., 2004. Angewandte Chemie International Edition 43, 6042–6108.
Kim, F., Song, J.H., Yang, P.D., 2002. Journal of the American Chemical Society 124, 14316–14317.
Lee, D.W., Park, K.M., Banerjee, M., Ha, S.H., Lee, T., Suh, K., Paul, S., Jung, H., Kim, J., Selvapalam, N., Ryu, S.H., Kim, K., 2011. Nature Chemistry 3, 154–159.
Li, H., Qiang, W.B., Vuki, M., Xu, D.K., Chen, H.Y., 2011. Analytical Chemistry 83, 8945–8952.
Lin, D.J., Wu, J., Yan, F., Deng, S.Y., Ju, H.X., 2011. Analytical Chemistry 83, 5214–5221.
Lu, D.L., Wang, J., Wang, L.M., Du, D., Timchalk, C., Barry, R., Lin, Y.H., 2011. Advanced Functional Materials 21, 4371–4378.
Malhotra, R., Patel, V., Vaque, J.P., Gutkind, J.S., Rusling, J.F., 2010. Analytical Chemistry 82, 3118–3123.
Mani, V., Chikkaveeraiah, B.V., Patel, V., Gutkind, J.S., Rusling, J.F., 2009. ACS Nano 3, 585–594.
Nie, H.G., Liu, L.S., Yu, R.Q., Jiang, J.H., 2009. Angewandte Chemie International Edition 48, 9862–9866.
Peng, J., Feng, L.N., Ren, Z.J., Jiang, L.P., Zhu, J.J., 2011. Small 7, 2921–2928.
Stoeva, S.I., Lee, J.S., Smith, J.E., Rosen, S.T., Mirkin, C.A., 2006. Journal of the American Chemical Society 128, 8378–8379.
Teng, Y.Q., Zhang, X.A., Fu, Y., Liu, H.J., Wang, Z.C., Jin, L.T., Zhang, W., 2011. Biosensors and Bioelectronics 26, 4661–4666.
Ting, B.P., Zhang, J., Khan, M., Yang, Y.Y., Ying, J.Y., 2009. Chemical Communications, 6231–6233.
Uhlenheuer, D.A., Petkau, K., Brunsveld, L., 2010. Chemical Society Reviews 39, 2817–2826.
Wang, J., Liu, G.D., Jan, M.R., 2004. Journal of the American Chemical Society 126, 3010–3011.
Wang, J., Liu, G.D., Wu, H., Lin, Y.H., 2008. Small 4, 82–86.
Wang, L.B., Zhu, Y.Y., Xu, L.G., Chen, W., Kuang, H., Liu, L.Q., Agarwal, A., Xu, C.L., Kotov, N.A., 2010. Angewandte Chemie International Edition 49, 5472–5475.
Wu, J., Fu, Z.F., Yan, F., Ju, H.X., 2007. Trends in Analytical Chemistry 26, 679–688.
Xia, F., Zuo, X.L., Yang, R.Q., Xiao, Y., Kang, D., Vallée-Bélisle, A., Gong, X., Yuen, J.D., Hsu, B.B., Heeger, A.J., Plaxco, K.W., 2010. In: Proceedings of the National Academy of Sciences of the United States of America 107, pp. 10837–10841.
Ye, X.C., Jin, L.H., Caglayan, H., Chen, J., Xing, G.Z., Zheng, C., Doan-Nguyen, V., Kang, Y., Engheta, N., Kagan, C.R., Murray, C.B., 2012. ACS Nano 6, 2804–2817.
Zhou, J., Zhuang, J.Y., Miró, M., Gao, Z.Q., Chen, G.N., Tang, D.P., 2012. Biosensors and Bioelectronics 35, 394–400.